The International Journal of Advanced Manufacturing Technology (2020) 106:1005–1015
https://doi.org/10.1007/s00170-019-04662-6

ORIGINAL ARTICLE

High-speed milling of CFRP composites: a progressive damage model of cutting force

Lifeng Zhang[1] · Sheng Wang[1] · Weilin Qiao[1] · Zhan Li[1] · Ning Wang[1] · Jin Zhang[1] · Tao Wang[1]

Received: 1 July 2019 / Accepted: 4 November 2019 / Published online: 3 December 2019

Abstract
Three-dimensional Hashin failure criterion and material stiffness degradation model were compiled by VUMAT subroutine. The Abaqus/Explicit solver was performed to establish progressive damage model of cutting force for CFRP high-speed milling, and high-speed milling experiments with different cutting parameters were carried out. Further, the impact mechanism of fiber cutting angle and cutting parameters on cutting force, stress, and material failure during milling was explored, and the material removal mechanism in high-speed milling of CFRP was revealed. The results show that the error between the experimental and simulated of cutting forces is less than 5%, which indicates that the progressive damage model is feasible. The fiber cutting angle has significant influence on cutting force and stress in cutting process, and the cutting direction has a significant influence on cutting force. In addition, cutting parameters play a critical role in cutting force, and the feed per tooth is the most significant factor affecting the cutting force. Simultaneously, the progressive damage model predicts that the shear failure of materials mainly concentrates in the cutting area and extends along the feed direction. Finally, the material removal mechanism of CFRP in high-speed milling was revealed combining cutting force experiment.

Keywords Progressive damage model · VUMAT subroutine · High-speed milling · Cutting force · Material removal mechanism

1 Introduction

Carbon fiber–reinforced plastic matrix composites (CFRPs) are widely applied in aerospace and other fields for its excellent characteristics such as light weight and high strength [1–3]. Especially, in the field of civil aviation, the composite coverage of Boeing and Airbus series aircraft has already exceeded 50%. The overall coverage of CFRP has become a trend in the future development of civil aviation aircraft [4, 5]. CFRP mainly adopts high-strength carbon fiber bundles to toughen and strengthen [6], and the milling is the common processing method of CFRP [7–9]. However, due to the complex weaved structure, the unclear failure mechanism, and the anisotropy of carbon fiber strength, the material removal mechanism in milling of CFRP is still unclear [10–12]. Besides, in the milling process of CFRP, it is very easy to produce defects such as material layering, burrs, surface pits, fibers breakage, and matrix cracks, which directly lead to poor processing efficiency and high cost [13–15], and then restrict the development of industry. Thus, the exploration of material removal mechanism in CFRP milling has become a vital issue in manufacturing industry.

With the increasing requirement of dimension, tolerance, and precision of aeronautical components and other high-precision products, research on cutting mechanism of CFRP is an important issue in mechanical manufacturing industry. The milling experiments of CFRP with different cutting parameters, fiber angles, and tool combination have been carried out by domestic and foreign scholars. The results show that cutting speed and fiber cutting angle have vital effect on the cutting force and material removal mechanism of CFRP milling [16–18]. Nevertheless, the cost of composite cutting experiment is too high, and it is intractable to monitor the material cutting process, cutting stress, and damage propagation state during the experiment. The great development of finite element simulation can well avoid the above shortcomings. Alessandro et al. [19] employed SPH method to establish a unidirectional CFRP cutting finite element model, and the cutting experiments were carried out to verify the reliability of the model. Various cohesion models were synthetically

✉ Tao Wang
farell772003@qq.com

[1] College of Aeronautical Engineering, Civil Aviation University of China, Tianjin 300300, China

considered by Essa et al. [20], and they established a model which can effectively avoid the excessive deformation of cohesion element in the simulation process. Su et al. [21] developed a three-dimensional finite element model of CFRP orthogonal shear, the strain of resin, and the different cutting angles of fiber were considered. Rao et al. [22] carried out a three-dimensional finite element model of CFRP cutting to investigate the impact of fiber cutting angle, cutting depth, and tool rake angle on cutting force. Feito et al. [23] completed the simplified model and complete model of CFRP drilling from the perspective of delamination prediction. Rentsch et al. [24] simulated the cutting process of CFRP with macro-model and micro-model. Xu et al. [25] established a finite element model of CFRP laser milling to consider the material removal mechanism, and the model could predict the ablation depth of the material during the laser milling process. The finite element model of anisotropic CFRP end milling was conducted by Ghafarizadeh et al. [26]. The cutting force, chip formation, and material damage mechanism in cutting process were discussed. Gao et al. [27] finished a three-dimensional micro-mechanical finite element model for CFRP processing. The model took into account the interfacial debonding between fibers/matrices and the heat transfer during composite failure. In summary, few studies on the finite element model of CFRP high-speed milling involve the progressive damage of material and failure expansion at present, so few discussions have been conducted on the progressive damage model of cutting force. Beyond this, few people systematically discuss the mechanism of material failure in high-speed milling of CFRP. The mechanism of the effect of fiber cutting angle on cutting force, cutting stress, and material removal mechanism is still unclear.

Based on three-dimensional Hashin failure criterion and material stiffness degradation model, a three-dimensional finite element model of progressive damage in unidirectional CFRP high-speed cutting was set up by compiling VUMAT subroutine and employing Abaqus/Explicit solver. Furthermore, the reliability of the model was verified by milling experiments with the identical parameters. The effect of fiber cutting angle on cutting force, cutting stress, material failure propagation and material removal mechanism was discussed. The research results can not only provide experimental basis for the investigation of processing mechanism of composites, but also improve the theory of high-speed machining of CFRP.

2 Progressive damage finite element model

2.1 Model setup

The Abaqus/Explicit module has significant advantages in solving the nonlinear dynamic process of composites cutting. At the moment, there are two central methods of composites modeling: the equivalent homogeneous three-dimensional solid model of macro-modeling, which achieves the anisotropic properties of composites by changing the coordinate system and changing the properties of materials in different orientations. Another is the microscopic cohesion model; the interface between fibers and matrices is directly presented in the model, which is primarily adopted to research the interface mechanics and delamination failure forms of materials. The primary purpose of this paper is to discuss the influence mechanism of fiber cutting angle on macroscopic cutting mechanism of CFRP. Meanwhile, the longtime of finite element calculation of cohesion model was considering. Therefore, the macro-modeling method of equivalent homogeneous three-dimensional entity was adopted. The material properties required for finite element modeling are shown in Table 1 [28]:

The tool model was defined as a rigid body with a tip radius of 0.03 mm. The rake angle and the clearance angle of the tool were 4°and 9°, respectively. Moreover, the elastic modulus was 860 GPa and Poisson's ratio was 0.078. To input cutting speed and output historical variables, a reference point was installed on the tool and was bound to all units of the tool. In order to compare with the milling experiment, the cutting parameters in the simulation used the same cutting speed as the actual milling. Besides, the cutting speed was 251.2 m/min and the cutting depth was 1 mm. The size and constraint settings of the finite element model are shown in Fig. 1, and the definition of fiber cutting angle is shown in Fig. 2. The cell type was C3D8R. Furthermore, the number of grids of cutting area was 118,000 and the mesh size was 10 μm. Furthermore, the bias ratio was set along the height direction of the material

Table 1 Performance parameters of unidirectional CFRP (T300) [28]

Type		Parameters
1- Modulus of elasticity	E_{11}	138.0 GPa
2- Modulus of elasticity	E_{22}	11 GPa
3- Modulus of elasticity	E_{33}	11 GPa
1-2 Poisson ratio	v_{12}	0.28
1-3 Poisson ratio	v_{13}	0.28
2-3 Poisson ratio	v_{23}	0.40
1-2 In-plane shear modulus	G_{12}	5.5 GPa
1-3 In-plane shear modulus	G_{13}	5.5 GPa
2-3 In-plane shear modulus	G_{23}	4.79 GPa
Density	ρ	1540.0 kg/m^3
1- Tensile strength	X_T	1500 MPa
1- Compressive strength	X_C	900 MPa
2- Tensile strength	Y_T	27 MPa
2- Compressive strength	Y_C	200 MPa
1-2 In-plane shear strength	S_{12}	80 MPa
1-3 In-plane shear strength	S_{13}	80 MPa
2-3 In-plane shear strength	S_{23}	60.5 MPa

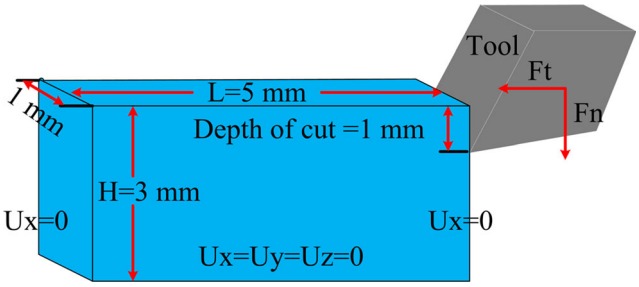

Fig. 1 The setting of finite element models and constraints

model. For the sake of reducing the calculation time and improve the accuracy of the model, the meshes were divided into more and more intensive from bottom to top. In other words, the number of meshes in the cutting area was larger.

2.2 VUMAT subroutine application

The three-dimensional Hashin failure criterion is suitable for failure analysis of composites, and its contents are shown in Table 2. In the actual cutting process, the tool tip will inevitably cause damage to the uncut area, which will result in the change of material properties to be cut. Consequently, the progressive damage model introduces material parameter degradation, and the specific material stiffness degradation rule is shown in Table 3.

The VAMUT subroutine was used to modify material constitutive relationship and material properties to achieve progressive damage cutting force model of CFRP. The three-dimensional Hashin failure criterion and material stiffness degradation model were programmed into VUMAT subroutine in the progressive damage model of high-speed milling. The implementation process of the subroutine is shown in Fig. 3. Firstly, the parameters were read from the three-dimensional material model, and then the strain values were obtained by calculating the elastic matrix. According to the three-dimensional Hashin failure criterion, the failure of the fiber and matrix could be judged. Assuming that no new element fails, the stress and strain values were directly returned to the main program. In contrast, if any element failed, the stiffness of the failed element was degraded and the stress was recalculated, and then the updated stress and strain were returned to the main program.

Table 2 Three-dimensional Hashin failure criteria

Type	Formula
Tensile failure of fiber	$\sigma_{11} > 0, \left(\frac{\sigma_{11}}{X_t}\right)^2 + \left(\frac{\sigma_{12}}{S_{12}}\right)^2 + \left(\frac{\sigma_{13}}{S_{13}}\right)^2 = 1$
Compression failure of fiber	$\sigma_{11} < 0, \left(\frac{\sigma_{11}}{X_c}\right)^2 = 1$
Tensile failure of matrix	$\sigma_{22} > 0, \left(\frac{\sigma_{22}}{Y_t}\right)^2 + \left(\frac{\sigma_{12}}{S_{12}}\right)^2 + \left(\frac{\sigma_{23}}{S_{23}}\right)^2 = 1$
Compression failure of matrix	$\sigma_{22} < 0, \left(\frac{\sigma_{22}}{Y_c}\right)^2 + \left(\frac{\sigma_{12}}{S_{12}}\right)^2 + \left(\frac{\sigma_{23}}{S_{23}}\right)^2 = 1$
Shear failure of fiber and matrix	$\sigma_{11} < 0, \left(\frac{\sigma_{11}}{X_c}\right)^2 + \left(\frac{\sigma_{12}}{S_{12}}\right)^2 + \left(\frac{\sigma_{13}}{S_{13}}\right)^2 = 1$

3 Experimental design

High-speed cutting technology can effectively reduce the cutting force of intractable materials such as CFRP and improve the processing efficiency. High-speed cutting mainly depends on the material performance and the actual linear speed in the cutting process. The experiments were carried out on DMU85 NC machining center, and the side milling and down milling were adopted within this paper. Unidirectional CFRP (T300, Toray) composites were employed as experimental materials, and three repeated experiments were carried out for each group of experimental parameters. As shown in Fig. 4, the unidirectional CFRP was cut into small cuboid specimens: 70 mm × 50 mm × 40 mm. The Kistler 9257A was located between the gripping device and the worktable. Further, the high-speed milling in four orientations was realized by rotating the worktable of the machining center. The specific experimental parameters are shown in Table 4.

4 Results and discussions

4.1 Effect of fiber cutting angle on cutting force

Figure 5 is a comparison of the experimental results and simulation results of cutting force in CFRP of high-speed milling. In the process of cutting, the change trend of cutting force experimental value and simulation value was consistent, and the error between experimental value and simulation value

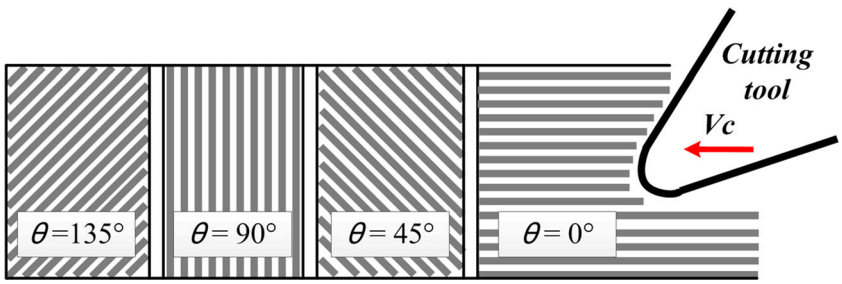

Fig. 2 The definition of fiber cutting angle

Table 3 Material stiffness degradation model [2]

Type	Material parameter degradation
Fiber tensile	$E = 0.07E$, $G = 0.07G$, $v = 0.07v$
Fiber compression	$E = 0.14E$, $G = 0.14G$, $v = 0.14v$
Matrix tensile	$E_{22} = 0.2E_{22}$, $G_{12} = 0.2G_{12}$, $G_{23} = 0.2G_{23}$
Matrix compression	$E_{22} = 0.4E_{22}$, $G_{12} = 0.4G_{12}$, $G_{23} = 0.4G_{23}$
Shear of fiber and matrix	$G_{12} = 0.1G_{12}$, $v_{12} = 0.1v_{12}$

was less than 5%, which reported that the cutting force model was reliable. The error was attributed to that although the material stiffness degradation model was set up in progressive damage model, the stiffness degradation followed the equation regularly. In the actual cutting process, the material damage near the tool front was not synchronous and irregular, which created the irregular degradation of material properties. Finally, there were errors between the values of experiments and simulations of cutting force.

Beyond this, both simulation and experimental results showed that the cutting force increased first and then decreased, especially the cutting force F_t and F_n followed the rule: $90° > 135° > 45° > 0°$. In the process of processing, the strength of resin was much lower than that of the carbon fibers, so the anisotropy of mechanical properties of carbon fibers was the dominant reason for the distinction of cutting forces. Section 4.7 will discuss in detail the main causes of the difference of cutting force.

4.2 Effect of fiber cutting angle on stress change in cutting process

Figure 6 is the cutting stress diagram of four orientations obtained by progressive damage model. As shown in Fig. 6 a, when cutting along the cutting angle of 0°, the cutting stress mainly concentrated near the tool tip and extended along the feed direction. This can be interpreted as that the main interfacial peeling of fibers occurred in the cutting material area under the load of cutting edge, while the fibers mainly overcame axial strength or shear strength to occur extrusion breakage in the uncut material area, and yet the interfacial debonding strength of CFRP was far less than the shear strength and axial strength of the fibers. There was also a stress concentration area near the rake face of the tool, which was

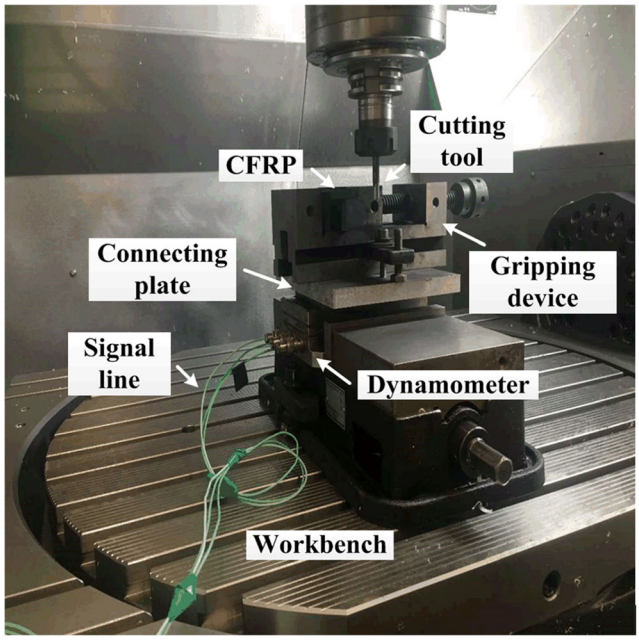

Fig. 4 The high-speed milling experiments of CFRP

caused by the high stress of the materials under the cutting and extrusion of the tool tip. When cutting along this orientation, the debonding failure of the fiber interface was the main cause of the composite removal, so the overall cutting stress was the minimum. Figure 6 b is a stress diagram of 45°orientation. The stress mostly concentrated on the tip of the tool. Concurrently, the fiber chiefly bore the shear force from the tip, while the shear resistance of fibers was weaker, so it was easy to be cut off directly. In reality, the difference of cutting stress in various fiber orientations was mostly caused by the anisotropy of fiber strength. Secondly, in the cutting process, diverse fiber orientations will lead to different cutting angles between the fiber axis and the tool tip. Thus, the cutting angles produced different forces and failure modes on the fibers. Then, fibers break in different modes and ultimately bring about unlikely cutting stress. For 45° orientation of fiber, the cutting tool primarily overcame the shear strength of the fibers, so the fibers were simple to be cut off and the cutting stress was small.

Figure 6 c is the stress diagram of the composite cutting along 90° cutting angle. The stress mostly distributed on the rake face of the tool, and the maximum stress occurred around the tool tip. The fiber bundles in the cutting area of the tool

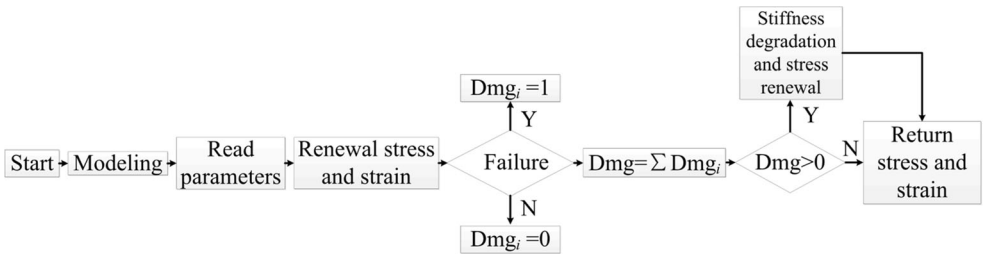

Fig. 3 The schematic diagram of subprogram

Table 4 Experimental parameters for high-speed milling

Type	Parameters
Fiber orientations (°)	0, 45, 90, 135
Spindle speed (r/min)	1000, 5000, 10,000, 15,000, 20,000
Cutting depth (mm)	0.5, 1, 1.5, 2, 2.5
Rake angle of tools (°)	4
Clearance angle of tools (°)	9
Feed per tooth (mm)	0.01, 0.02, 0.03, 0.04, 0.05
Tool diameter (mm)	8
Milling cutter type	PCD tool
Tool edge	2
Milling machine	DMU85

rake face were perpendicular to the cutting orientation, and part of the fiber bundles would be cut directly under the shear action of the tool. Nevertheless, due to the high elongation at break of carbon fibers, the fibers were extruded and deformed by the tool tips; thus, the fibers would be subjected to the tensile stress of the cutting tool. There will be severe friction in the second deformation zone during cutting. Only when the axial strength of the fibers was overcome, the fibers would break. Hence, the cutting stress was the sum of shear stress and tensile stress of the fiber bundles when cutting along this cutting angle, so the cutting stress was the maximum in this orientation. Figure 6 d is the stress diagram of cutting along the cutting angle of 135°. The cutting stress mainly concentrated under the tool, and the stress range was large. Most of the fibers would be lifted under the bending pressure of the tool. When the applied bending stress exceeded the bending strength of the fibers, brittle fracture occurred. Furthermore, some fiber bundles were subjected to the load of cutting edge directly in the axial direction. When the load reached the maximum of axial strength of the fiber, the fiber also broke and crushed, and then removed. Therefore, the cutting stress was larger. It can also be acquired from Fig. 6 that the main stress concentration area (the white dotted frame selected area in the figure) was consistent with the orientation of the fiber, which was determined by the fact that the axial strength of the fiber was above the strength of other orientations. Furthermore, the stress in cutting process followed the rule 90° > 135° > 45° > 0°, which was consistent with the rule of cutting force.

4.3 Effect of fiber cutting angle on material failure during cutting process

Previous studies have shown that shear failure of fibers is the main material removal mode in composite cutting process [21]. Figure 7 shows the fiber-matrix shear failure during high-speed cutting of CFRP obtained by the progressive damage model. Sdv1 is shear failure of the fiber and matrix. The red grid in the figure represents the failure grid and the blue grid represents the no failure. In particular, the initial failure of the composites was considered at the 135° orientation. When the tool touched the composites, the shear failure extended in a long and narrow shape along the feed direction of the tool to the materials, and the failure expanded gradually in the form of continuity.

The results of shear failure in high-speed cutting of CFRP are shown in Fig. 8. The cutting area of tool is defined above the white dotted line and the non-cutting area below the white dotted line. As shown in Fig. 8 a, shear failure primarily extended along the *X* direction (feed direction of the tool) when cutting along the orientation of 0°, and the failure mainly concentrated in the cutting area. Figure 10 b shows the shear failure propagation law when cutting along 45° orientation.

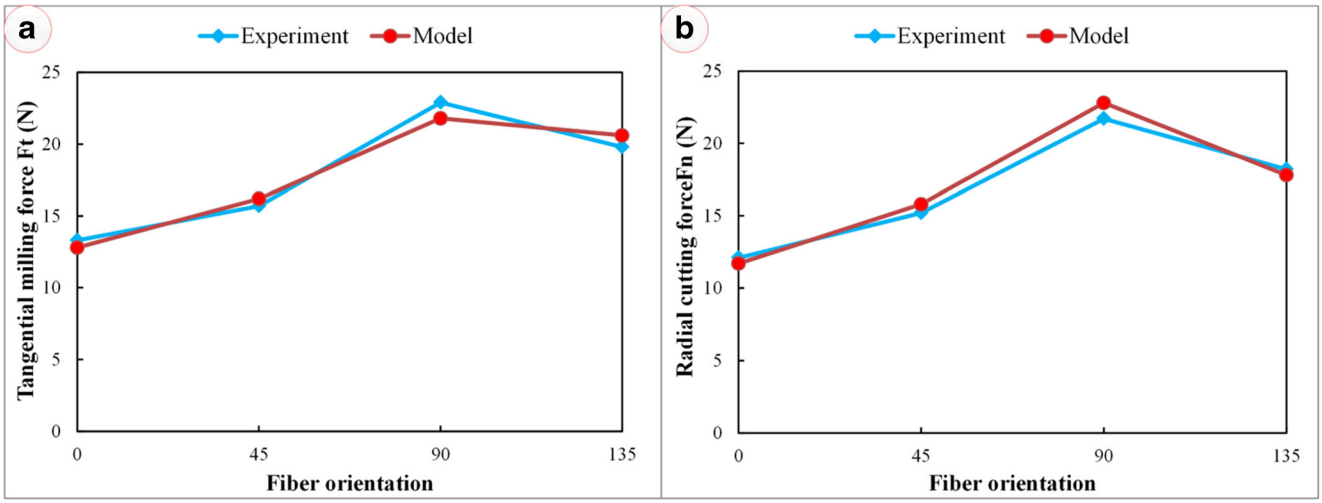

Fig. 5 The results of experiment and model. Fiber cutting angle (v_s = 10,000 r/min, f_z = 0.03 mm, a_e = 1 mm)

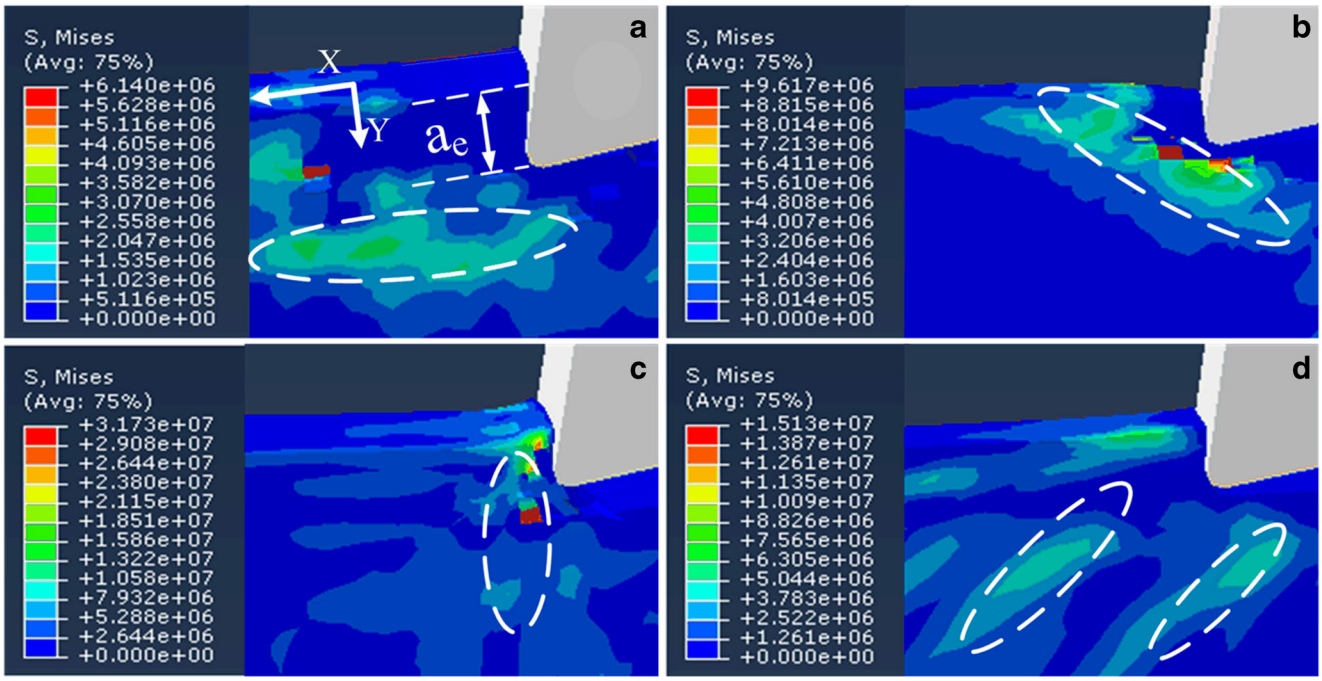

Fig. 6 The effect of fiber orientation on cutting stress

The failure primarily extended along the X direction, and a small part of the failure occurred in the non-cutting area. As shown in Fig. 10 c, the shear failure mostly occurred in the cutting area of the tool and extended along the X direction. When cutting along this orientation, the failure range was the largest, and more failure occurred in the non-cutting area. Figure 10 d shows the extension rule of the shear failure when cutting along the 135° orientation. The shear failure primarily occurred on the upper surface of the material in the cutting area, and the failure range was the minimum. Generally speaking, progressive damage model pointed out that the direction of shear failure propagation was mostly X direction, and the failure mainly concentrated in the cutting area of the tool in the process of CFRP high-speed cutting. The shear failure was most likely to occur in 90° orientation, and the failure range of 135° orientation was the minimum. In the cutting process of composites, material failure mode has a major effect on the cutting force.

4.4 Effect of spindle speed on cutting force

Figure 9 shows the effect of spindle speed on cutting force in high-speed milling of CFRP when the cutting depth was 1.5 mm and the feed per tooth was 0.03 mm. As shown in Fig. 9 a, the average tangential force F_t increased first and then decreased, and when the spindle speed exceeded 10,000 r/min, the cutting force F_t decreased and tended to be stable. The results showed that the tangential force of CFRP milling process could be reduced by high-speed milling in a certain range. However, the effect of cutting force reduction in high-speed cutting was not obvious. Taking 90° cutting angle as an example, cutting force was reduced from 23.6 N (10,000 r/min) to 23 N (20,000 r/min) by high-speed cutting. This was because the strength of the plastic matrix was too low, and the cutting force was mainly composed of the force overcome by the removal of fiber deformation and the friction force. The fiber was brittle material, because of its small plastic

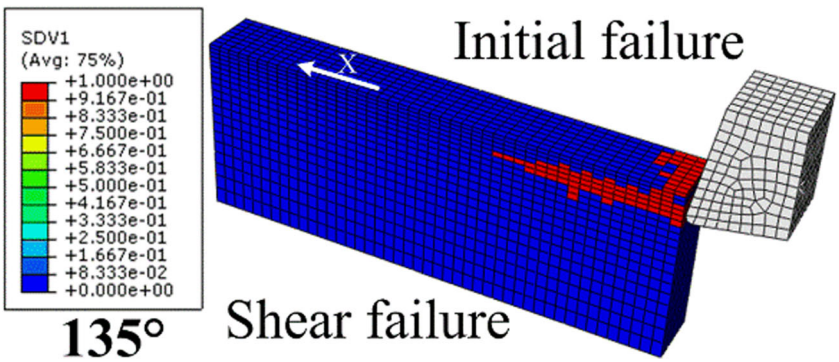

Fig. 7 The progressive damage of the shear failure in 135° orientation

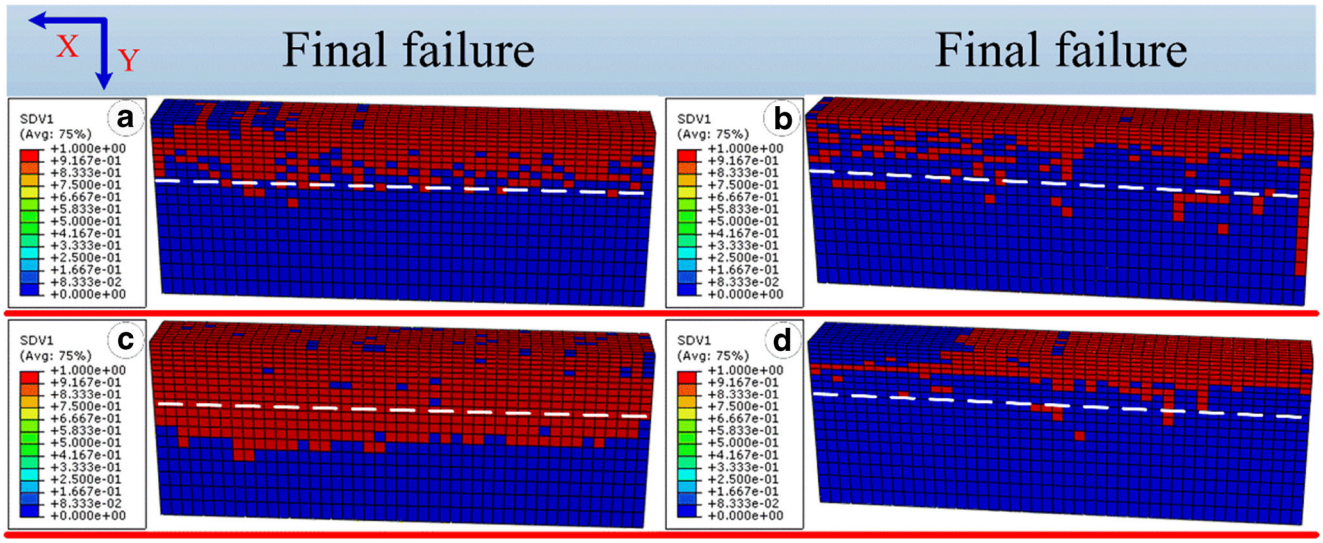

Fig. 8 The progressive damage of the shear failure in four orientations

deformation, little friction between chips, and rake face of tool. In the process of continuous cutting, cutting speed had no significant effect on the change of cutting force, so in the range of spindle speed from 10,000 to 20,000 r/min, the change of cutting force was unapparent, and the trend of change was gradually stable. Figure 9 b shows the trend of the impact of spindle speed on the average radial force F_n in CFRP high-speed milling. Unlike the average tangential force F_t, the average radial force F_n increased with the spindle speed in cutting process. Actually, according to the cutting mechanism and milling force characteristics, the radial cutting force mainly reflected the rebound of the cutting material. With the increase of spindle speed, the extrusion speed of the tool flank face to the machined surface increased, so the radial force F_n would increase. In addition, the narrow pulse width and high frequency of milling force would cause distortion of measurement signal, and increase the peak value of cutting force signal at high speed. When cutting along four orientations, F_n was smaller in the low-speed section, and the maximum radial force was only 1.3 times of the minimum radial force, and the change of radial force was not obvious in the cutting process.

From the comprehensive analysis of tangential force and radial force in cutting process, it can be concluded that high-speed milling has a significant impact on the tangential force. In fact, in the process of side milling, the force required for material removal mostly comes from the tangential force F_t which is consistent with the feed direction (X direction). Therefore, the tangential force is defined as the main cutting force in this paper. Next, the main cutting force in the process of high-speed milling of CFRP was discussed.

4.5 Effect of cutting depth on cutting force

The effect of cutting depth on the main cutting force F_t was discussed under the condition of spindle speed of 10,000 r/

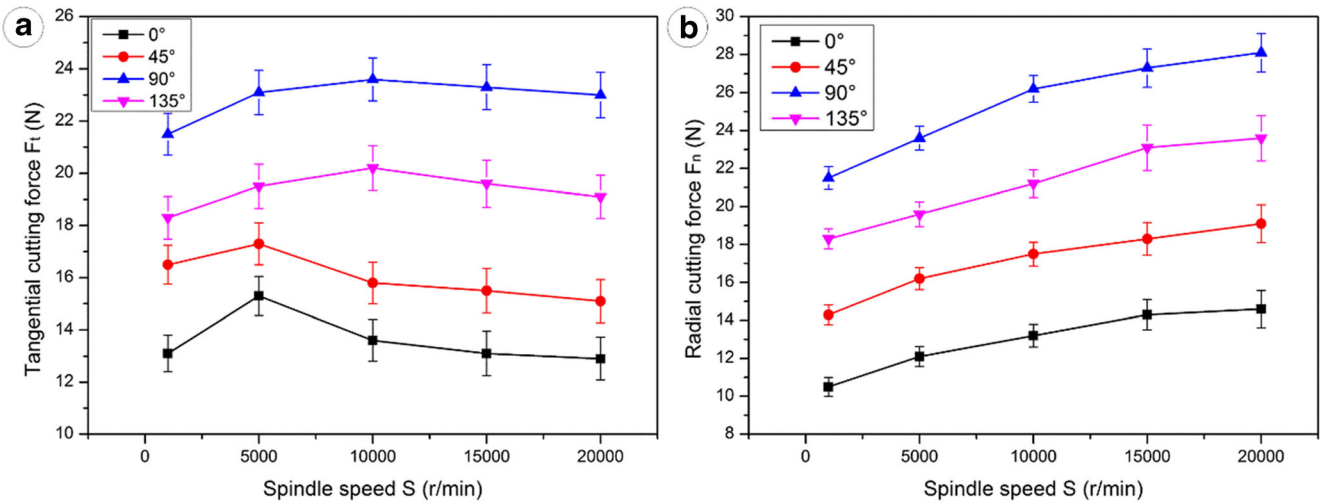

Fig. 9 The effect of spindle speed on cutting force. Spindle speed ($f_z = 0.03$ mm, $a_e = 1.5$ mm)

min and feed per tooth of 0.02 mm. As shown in Fig. 10, the main cutting force increased with the cutting depth. The main cutting force varied greatly with the cutting depth when cutting along 90° and 135° orientations. Specifically, the main cutting force increased from 16.3 to 27.1 N for 90° orientation. When cutting along 45° and 0° orientations, the change of main cutting force was minor. Particular in 0° orientation, the change of main cutting force was the minimum, and the maximum value of cutting force was only 1.4 times of the minimum value. The results illustrated that the impact of cutting depth on the main cutting force was unlikely when cutting along the various fiber cutting angles, and the most significant change was the 90° orientation. Besides, when the radial cutting depth increased to 1.5 mm, the change of the main cutting force was not obvious, but tended to be stable. This can be explained by the maximum milling thickness h_m and the expression of h_m is as follows:

$$h_m \approx f_z \sqrt{\frac{a_e}{D}} \tag{1}$$

where h_m is the maximum milling thickness, f_z is the feed per tooth, a_e is the radial cutting depth, and D is the tool diameter. Equation (1) showed that h_m was proportional to a_e when the f_z and D were fixed. Since the nature of power function, when the radial cutting depth increased to a certain value, the trend of effect on milling force began to weaken, which was consistent with the trend in Fig. 10.

4.6 Effect of feed per tooth on cutting force

Figure 11 shows the relationship between the feed per tooth and the main cutting force when the spindle speed was 10,000 r/min and the cutting depth was 1 mm. The main cutting force in four orientations increased with the feed per tooth. Especially, with the increase of feed per tooth, the cutting force increased by about 12 N and 8 N in 135° and 0° respectively. The results illustrated that the influence of feed per tooth on the main cutting force was unequal when cutting along different orientations of fibers. The central reason for diversity was that the volume of material removed by cutting edge varied in unit time with the increase of feed per tooth. The anisotropy of mechanical properties of fibers in removal of materials was the dominant factor for the distinctness of main cutting forces. In the meantime, the three diagrams showed that the cutting force in high-speed milling of CFRP accorded with the rule of 90° > 135° > 45° > 0°, which was consistent with the conclusion of Section 4.1.

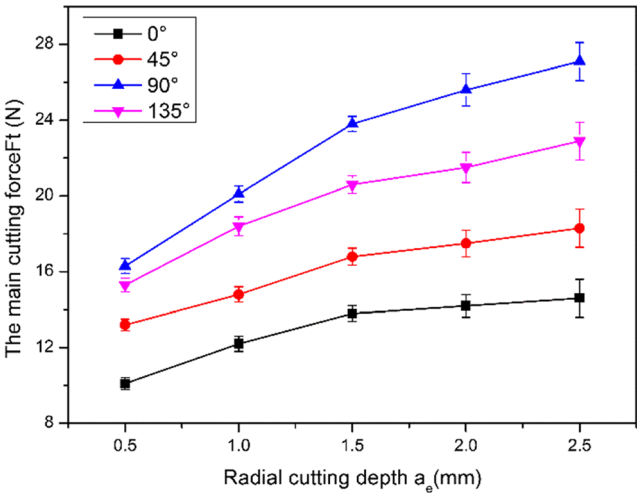

Fig. 10 The effect of cutting depth on main cutting force. Radial cutting depth (v_s = 10,000 r/min, f_z = 0.02 mm)

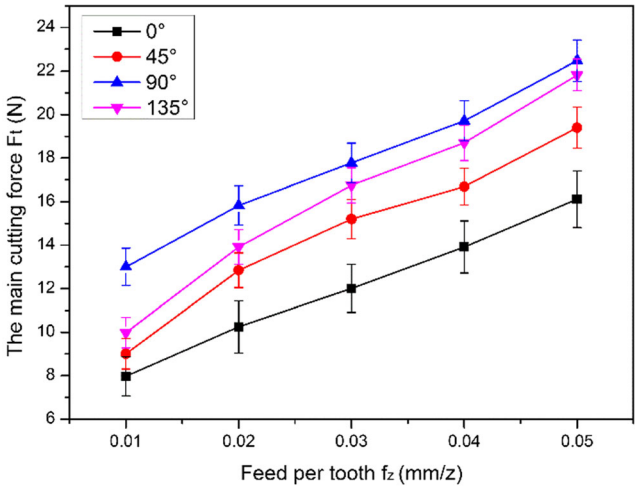

Fig. 11 The effect of feed per tooth on main cutting force. Feed per tooth (v_s = 10,000 r/min, a_e = 1 mm)

4.7 Material removal mechanism analysis

Fiber cutting angle plays an important role in material removal mechanism of CFRP high-speed milling. Cutting mechanism is especially complicated on account of the weave structure of composites, the anisotropy of mechanical properties of fibers, and the difference of properties between fibers and matrices. Moreover, the strength of fibers is far exceeding the strength of plastic matrices, so the removal of fibers during cutting is the essential factor for the diversity of cutting forces. In addition, the anisotropy of fibers leads to different friction coefficients in four directions. The difference of fiber mechanics and friction performance in typical directions is the main reason for the change of cutting force [29]. Figure 12 illustrates the material removal mechanism in CFRP high-speed milling with four fiber orientations.

As shown in Fig. 12 a, at a fiber cutting angle of 0°, the crack mainly propagates along the fiber axis under the dynamic impact of cutting tools. Because the interfacial strength between fibers and matrix is far less than that of fibers, it is easier for fibers and matrices to debond; thus, the material of cutting layer and matrix material are continuously separated.

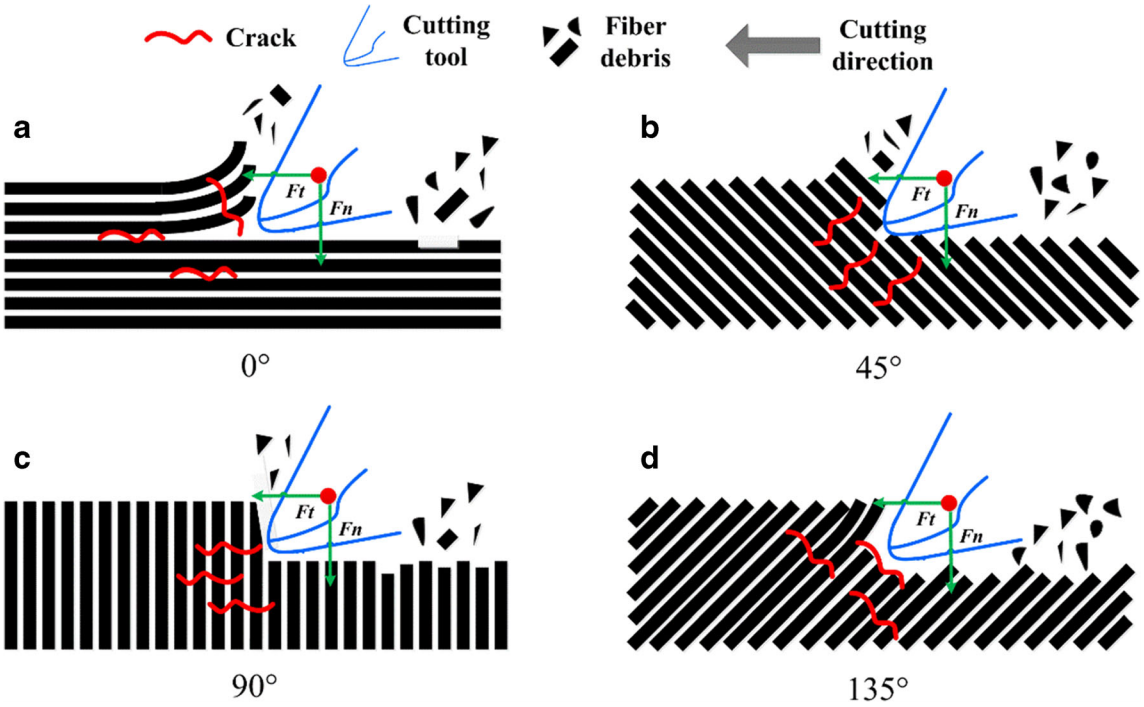

Fig. 12 Material removal mechanism in high-speed milling of CFRP

When continuing to apply load, the cutting material is continuously extruded. When the extrusion accumulates to a certain extent, the cutting material bends and is lifted up. In this process, the fibers mainly bear bending stress. When the applied load exceeds the strength of the material itself, the bending part separates from the material body and finally forms chips. When cutting along this orientation, the cutting force is the minimum.

Figure 12 b is a schematic diagram of CFRP material removal mechanism for 45°. The shear stress perpendicular to the axis of the fiber is formed by the extrusion of the tool on the composites. When the shear stress exceeds the shear strength limit of the fibers, the fibers are cut off. The fibers are mainly subjected to the shear action of cutting edges. Due to the low shear strength of the fibers, the fibers are easily cut off. The broken fibers slip along the cutting edge and form chips owing to the pushing of the cutting edge.

As shown in Fig. 12 c, when cutting along 90°orientation, cracks primarily occur in front of the tool and propagate along the feed direction. In the cutting process, the maximum stress occurs at the tool tip. Under the cutting and extrusion of the tool, the fiber is stretched and deformed. Actually, the tensile strength of the fibers is far exceeding the shear strength, and the shear failure of the fibers is easy. In virtue of the high elongation at break of fibers, the ultimate shear failure of fibers is caused by cutting forces. When cutting in this orientation, the cutting force is the maximum.

Figure 12 d is a material removal mechanism diagram for the cutting angle of 135°. On account of the radius of the blunt circle of tool, under the cutting and extrusion of the tool, the maximum stress is not at the tool tip, but at the maximum bending stress concentration point below the tool tip. During the cutting process, with the increase of cutting force, the extrusion deformation of the cutting tool on the front material increases, and the bending stress of the fiber enlarges gradually. Simultaneously, the crack initiates and propagates along the radial direction of the fiber. When the shear strength limit of the material is reached, the shear failure of the fibers results in a serrated profile on the surface of the composites.

In the process of CFRP cutting, the brittle fracture of carbon fibers and plastic removal of matrices were dominantly occurred. On the other hand, when cutting along various orientations of fibers, the shear failure of fibers under the combined action of cutting forces is the essential factor for material removal. Owing to the anisotropy of the mechanical properties of the fibers, the cutting forces are significantly distinct in all orientations.

5 Conclusions

In this paper, the progressive damage finite element model of cutting force in high-speed milling of CFRP was established by employing Abaqus/Explicit solver and VAMUT subroutine. The experiments of high-speed milling with various parameters were carried out. Ultimately, the effects of fiber cutting angle and cutting parameters on cutting force and material removal mechanism were predominantly considered. The main conclusions were as follows:

(1) The three dimensional Hashin failure criterion and material stiffness degradation model were compiled into VUMAT subroutine, and a progressive damage model of cutting force for CFRP high-speed cutting was achieved. Then, a series of cutting experiments were carried out to verify the model, and the error value experiments and simulations were less than 5%. It showed that the model was credible and could predict cutting force, stress concentration, and material failure in the process of CFRP cutting.

(2) The progressive damage model and cutting force experiments showed that the cutting angle of fiber had a significant impact on cutting force, stress, and material failure in CFRP high-speed milling. The cutting force and stress followed the rule $90° > 135° > 45° > 0°$. Moreover, progressive damage model predicted that the shear failure mainly occurred in the cutting area and extended along the X direction. The maximum range of failure occurred in the 90° orientation and the minimum was in the 135°.

(3) Cutting parameters played a critical role on cutting force. With the increase of spindle speed, tangential cutting force increased first, then decreased and tended to be stable. Yet the radial cutting force increased slowly with the increase of spindle speed. The main cutting force increased with the feed per tooth and radial cutting depth. In the process of high-speed milling of CFRP, cutting parameters had different effects on cutting forces in distinct fiber cutting angles, and the feed per tooth was the most significant factor.

(4) Based on the anisotropy of mechanical properties of fibers, the material removal mechanism of CFRP cutting was revealed. The anisotropy of mechanical properties of fibers brought about different removal forms, which was the main reason for the diversity of cutting forces. Under the load of cutting tools, the fibers mainly occurred shear failure and brittle removal.

Funding information This study received financial support from the Fundamental Research Funds for the Central Universities (No. 3122018C007), the National Natural Science Foundation of China (No. 51705518), the United National Science Funds and Civil Aviation Funds (No. U1633104), and the Open Funds of the State Key Lab of Digital Manufacturing Equipment and Technology (No. DMETKF2017018).

References

1. Geier N, Szalay T, Takács M (2019) Analysis of thrust force and characteristics of uncut fibres at non-conventional oriented drilling of unidirectional carbon fibre-reinforced plastic (UD-CFRP) composite laminates. Int J Adv Manuf Technol 100(9–12):3139–3154
2. Liu WS, He ZP, Yu F, Qing GH (2019) A progressive damage model introducing temperature field for bolted composite joint with preload. Model Simul Mater Sci Eng 27(6):065011
3. Li H, Qin XD, He GY, Jin Y, Sun D, Price M (2016) Investigation of chip formation and fracture toughness in orthogonal cutting of UD-CFRP. Int J Adv Manuf Technol 82(5–8):1079–1088
4. Ahmad J (2009) Machining of polymer composites. Springer pages 75–77
5. Oh S, Lee I, Park YB, Ki H (2019) Investigation of cut quality in fiber laser cutting of CFRP. Opt Laser Technol 113:129–140
6. Gara S, Tsoumarev O (2016) Effect of tool geometry on surface roughness in slotting of CFRP. Int J Adv Manuf Technol 86(1–4): 451–461
7. Geier N, Szalay T (2017) Optimisation of process parameters for the orbital and conventional drilling of unidirectional carbon fibre-reinforced polymers (UD-CFRP). Measurement 110:319–334
8. Sui J, Wang C (2019) Machinability study of unidirectional CFRP laminates by slot milling. Int J Adv Manuf Technol 100(1–4):189–197
9. He YL, Qing HN, Zhang SG, Wang DZ, Zhu SW (2017) The cutting force and defect analysis in milling of carbon fiber-reinforced polymer (CFRP) composite. Int J Adv Manuf Technol 93(5–8):1829–1842
10. Karpat Y, Bahtiyar O, Değer B (2012) Mechanistic force modeling for milling of unidirectional carbon fiber reinforced polymer laminates. Int J Mach Tools Manuf 56:79–93
11. Ozkana D, Goka MS, Ogea M, Karaoglanli AC (2018) Milling behavior analysis of carbon fiber-reinforced polymer (CFRP) composites. Mater Sci 2214(7853):2019
12. Calzada KA, Kapoora SG, DeVor RE, Samuel J, Srivastava AK (2012) Modeling and interpretation of fiber orientation-based failure mechanisms in machining of carbon fiber-reinforced polymer composites. J Manuf Process 14(2):141–149
13. Li H, Qin XD, Huang T, Liu XP, Sun D, Jin Y (2018) Machining quality and cutting force signal analysis in UD-CFRP milling under different fiber orientation. Int J Adv Manuf Technol 98(9–12): 2377–2387
14. Wang F, Yin J, Ma J (2017) Effects of cutting edge radius and fiber cutting angle on the cutting-induced surface damage in machining of unidirectional CFRP composite laminates. Int J Adv Manuf Technol 91(9–12):3107–3120
15. Geier N, Szalay T, Biró I (2018) Trochoid milling of carbon fibre-reinforced plastics (CFRP). Procedia CIRP 77:375–378
16. Wang C, Liu G, An Q (2017) Occurrence and formation mechanism of surface cavity defects during orthogonal milling of CFRP laminates. Compos Part B-Eng 109:10–22
17. Hintze W, Cordes M, Koerkel G (2015) Influence of weave structure on delamination when milling CFRP. J Mater Process Tech 216:199–205
18. Chen Y, Guo X, Zhang K (2019) Study on the surface quality of CFRP machined by micro-textured milling tools. J Manuf Process 37:114–123
19. Abena A, Essa K (2019) 3D micro-mechanical modelling of orthogonal cutting of UD-CFRP using smoothed particle hydrodynamics and finite element methods. Compos Struct
20. Abena A, Soo SL, Essa K (2017) Modelling the orthogonal cutting of UD-CFRP composites: development of a novel cohesive zone model. Compos Struct 168:65–83
21. Su Y (2019) Effect of the cutting speed on the cutting mechanism in machining CFRP. Compos Struct 220:662–676
22. Rao GVG, Mahajan P, Bhatnagar N (2008) Three-dimensional macro-mechanical finite element model for machining of unidirectional-fiber reinforced polymer composites. Mat Sci Eng A-Struct 498(1–2):142–149
23. Feito N, López-Puente J, Santiuste C (2014) Numerical prediction of delamination in CFRP drilling[J]. Compos Struct 108:677–683
24. Rentsch R, Pecat O, Brinksmeier E (2011) Macro and micro process modeling of the cutting of carbon fiber reinforced plastics using FEM. Procedia Eng 10:1823–1828

25. Xu H, Hu J (2017) Modeling of the material removal and heat affected zone formation in CFRP short pulsed laser processing. Appl Math Model 46:354–364
26. Ghafarizadeh S, Chatelain JF, Lebrun G (2016) Finite element analysis of surface milling of carbon fiber-reinforced composites. Int J Adv Manuf Technol 87(1–4):399–409
27. Gao C, Xiao J, Xu J (2016) Factor analysis of machining parameters of fiber-reinforced polymer composites based on finite element simulation with experimental investigation. Int J Adv Manuf Technol 83(5–8):1113–1125
28. Soden P D, Hinton M J, Kaddour A S (2004) Lamina properties, lay-up configurations and loading conditions for a range of fibre reinforced composite laminates//failure criteria in fibre-reinforced-polymer composites. Elsevier: 30-51
29. Chakladar ND, Mandal P, Potluri P (2014) Effects of inter-tow angle and tow size on carbon fibre friction. Compos Part A-Appl S 65:115–124